Open Journal of Acoustics, 2015, 5, 218-225
Published Online December 2015 in SciRes. http://www.scirp.org/journal/oja
http://dx.doi.org/10.4236/oja.2015.54017

Diameter Dependent Ultrasonic Characterization of InAs Semiconductor Nanowires

Mohit Gupta[1*], Punit K. Dhawan[1], Satyendra Kumar Verma[2], Raja Ram Yadav[1]

[1]Department of Physics, University of Allahabad, Allahabad, India
[2]Government Polytechnic, Gonda, India
Email: [*]mohitauphy89@gmail.com

Received 2 December 2015; accepted 26 December 2015; published 29 December 2015

Abstract

In this paper, we report the diameter dependent ultrasonic characterization of wurtzite structured InAs semiconductor nanowires at the room temperature. In this work, we have calculated the non-linear higher order elastic constants of InAs nanowires validating the interaction potential model. The ultrasonic attenuation and velocity in the nanowires are determined using the elastic constants for different diameters of the nanowires. Where possible, the results are compared with the experiments. Finally, we have established the correlation between the size dependent thermal conductivity and the ultrasonic attenuation of the nanowires.

Keywords

Ultrasonic Attenuation, Nanowires, Elastic Constants, Thermal Relaxation Time, Thermal Conductivity

1. Introduction

The small band gap of semiconducting Indium Arsenide nanowires (InAs NWs) is 0.35 eV and its electron mobility is high due to its small electron effective mass. InAs NWs have the highest thermoelectric figure of merit (ZTs) of all III-V NWs. Due to all these properties, InAs NWs have attracted a tremendous amount of interest and also have been a hot topic in recent years. Much of it is due to their potential applications in various fields such as biosensors [1] [2], field-effect transistors [3]-[6], light-emitting diodes [7], diode lasers and infrared detectors [8]-[10], logic gates [11], photo detectors [12] [13], solar cells [14], ultrahigh-density memory and logic devices [5] and thermoelectric devices. Additionally, heterostructures in one-dimensional geometries such as

[*]Corresponding author.

How to cite this paper: Gupta, M., Dhawan, P.K., Verma, S.K. and Yadav, R.R. (2015) Diameter Dependent Ultrasonic Characterization of InAs Semiconductor Nanowires. *Open Journal of Acoustics*, **5**, 218-225.
http://dx.doi.org/10.4236/oja.2015.54017

NWs have been to act as high performance function building blocks in devices.

A special feature is that it is possible to grow InAs NWs with hexagonal wurtzite (WZ) structure, which is non-existing in the corresponding bulk materials where the cubic zinc blende (ZB) structural modification prevails. Thus InAs NWs exhibits both a WZ phase as well as a ZB phase while InAs crystals typically exhibit ZB phase [15] [16]. For InAs NWs, in the WZ phase, each atom is tetrahedrally coordinated with ABAB stacking sequence, which is similar to the ZB phase. The nearest neighbor arrangement for each atom in the WZ phase is the same as that for the ZB phase, which is achieved when the c/a is 1.633. In fact, the <111> direction for the ZB phase is equivalent to the <001> direction of the WZ phase [17].

The previous studies concerning crystal structure also suggest that the InAs NWs with the smallest diameters have the WZ phase while the NWs with larger diameters have the ZB phase. For the intermediate diameters, the NWs consist of alternating segments of the two crystal phases [18]. However, the growth of WZ phase InAs NWs has been demonstrated using chemical beam epitaxy (CBE) [19] [20] and other techniques. The synthesis of these WZ phase InAs NWs resulted in extensive interest within the research fields to determine how their electrical and thermal transport properties are compared to those of ZB phase InAs NWs. However, while a significant amount of theoretical and experimental work has been focused on investigating mechanical, thermal, electrical and optical properties of InAs NWs in their WZ phase but none of the work reported in the literature so far is focused on the ultrasonic characterization of the InAs NWs. The ultrasonic evaluation method is very simple, non-radiative and non-destructive characterization method to predict the microstructural behavior and the thermophysical properties.

In view of this background, in the present work, we have calculated second and third order elastic constants, ultrasonic attenuation, and ultrasonic velocity along with related non-linear parameters in InAs NWs at 300 K aiming to the nondestructive characterization of the materials and establishment of the theories for the calculation.

2. Acoustic Theory of Wurtzite Structured Materials

2.1. Higher-Order Elastic Constants

The interaction potential called Lennard-Jones potential, $\varphi(r)$, used to calculate the higher-order elastic constants of WZ structured materials is given as:

$$\varphi(r) = -\frac{a_0}{r^m} + \frac{b_0}{r^n} \tag{1}$$

where; a_0, b_0 are constant scientific parameters; m & n are integers and r is distance between atoms [21]. The meaning may be understood as follows:

$$\eta = nb_0(n-m)/2MD^{n+2}$$

where η is the lagrangian strain, M is the mass of the atom and $D = a_0$ is the nearest neighbour distance in the basal plane.

K_2 is the harmonic parameter which is related to η as $K_2 = \dfrac{1}{4(\eta M/D^2)}$ Further, b_0 is the fitting parameter determined under the equilibrium condition for minimum system energy [22].

Developing the interaction potential model second and third order elastic constants (SOECs and TOECs) can be calculated by the equations [23] [24] as:

$$\left.\begin{array}{ll}
C_{11} = 24.1\,p^4C' & C_{12} = 5.918\,p^4C' \\
C_{13} = 1.925\,p^6C' & C_{33} = 3.464\,p^8C' \\
C_{44} = 2.309\,p^4C' & C_{66} = 9.851\,p^4C' \\
C_{111} = 126.9\,p^2B + 8.853p^4C' & C_{112} = 19.168\,p^2B - 1.61\,p^4C' \\
C_{113} = 1.924\,p^4B + 1.155p^6C' & C_{123} = 1.617p^4B - 1.155p^6C' \\
C_{133} = 3.695p^6B & C_{155} = 1.539p^4B \\
C_{144} = 2.309p^4B & C_{344} = 3.464p^6B \\
C_{222} = 101.039p^2B + 9.007p^4C' & C_{333} = 5.196p^6B
\end{array}\right\} \tag{2}$$

where $p = c/a$ is called axial ratio; $C' = \chi a/p^5$; $B = \psi a^3/p^3$; $\chi = 1/8\left[\left\{nb_0(n-m)\right\}/\left\{a^{n+4}\right\}\right]$; $\Psi = -\chi/\left\{6a^2(m+n+6)\right\}$; and c is height of the unit cell. The harmonic and anharmonic parameters (χ and ψ) are calculated using one reasonable value of SOECs. The basal plane distance, axial ratio collectively called lattice parameters [25] are a = 4.284 Å and p = 1.633.

2.2. Ultrasonic Velocities

The anisotropic properties of a material are related to its ultrasonic velocities as they are related to higher-order elastic constants. If ultrasonic wave is propagating along the length of the NWs then there are two types of ultrasonic velocities: one longitudinal and other shear wave velocities [26] [27] which are given by following equations:

$$v_L = \left(C_{33}/\rho\right)^{1/2} \tag{3}$$

$$v_S = \left(C_{44}/\rho\right)^{1/2} \tag{4}$$

where v_L and v_S are the longitudinal and shear wave velocities while ρ is the mass density of the material.

2.3. Ultrasonic Attenuation and Allied Parameters

The main causes for the ultrasonic attenuation in solid are electron-phonon interaction, phonon-phonon interaction, grain boundary loss or scattering loss, Bardoni relaxational loss and thermoelastic loss. The electron mean free path is not comparable to phonon wavelength at high temperature; therefore attenuation due to electron-phonon interaction will be absent. Scattering loss is prominent for polycrystalline material and it has no role in case of single crystals. Bardoni relaxational loss has been found to be effective at low temperature for metals. So, two dominant processes responsible for the ultrasonic attenuation at high temperature are phonon-phonon interaction also known as Akhieser loss and thermo-elastic attenuation. The ultrasonic attenuation coefficient $(\alpha)_{Akh}$ (Akhieser type loss) due to phonon-phonon interaction mechanism is given by following expression [27]:

$$\left(\alpha/f^2\right)_{Akh} = 4\pi^2\left(3E_0\left\langle\left(\gamma_i^j\right)^2\right\rangle - \left\langle\gamma_i^j\right\rangle^2 C_V T\right)\tau\Big/2\rho V^3 \tag{5}$$

where f is the frequency of the ultrasonic wave; V is the velocity for longitudinal and shear waves as defined in the set of Equations (3); E_0 is the thermal energy density [28] and C_V is the specific heat per unit volume of the material [28]; T is the temperature and γ_i^j is the Grüneisen number; i and j are the mode and direction of the propagation. The Grüneisen number for a hexagonal WZ structured crystal along the <001> orientation is a direct consequence of the SOECs and TOECs. The acoustic coupling constant "D" is the measure of the acoustic energy converted into thermal energy given by the equation as:

$$D = 3\left(3E_0\left\langle\left(\gamma_i^j\right)^2\right\rangle - \left\langle\gamma_i^j\right\rangle^2 C_V T\right)\Big/E_0 \tag{6}$$

when an ultrasonic wave propagates through a crystalline material, the equilibrium of phonon distribution is disturbed. The time taken for re-establishment of equilibrium of the thermal phonons is called the thermal relaxation time "τ" and it is given as:

$$\tau = \tau_S = \tau_L/2 = 3K/C_V V_D^2 \tag{7}$$

where τ_L is the thermal relaxation time for the longitudinal wave; τ_S is the thermal relaxation time for the shear wave; and K is the thermal conductivity [29]; V_D is the Debye average velocity calculated by the equation as:

$$v_D = \left[\frac{1}{3}\left(\frac{1}{v_L^3} + \frac{2}{v_S^3}\right)\right]^{-1/3} \tag{8}$$

The propagation of the longitudinal ultrasonic wave results in the thermoelastic loss "$(\alpha)_{Th}$" due to creation of compressions and rarefactions throughout the lattice and it is calculated by the equation [27] as:

$$\left(\alpha/f^2\right)_{Th} = 4\pi^2 \left\langle \gamma_i^j \right\rangle^2 KT/2\rho V_L^5 \tag{9}$$

The thermoelastic loss for the shear wave has no physical significance because the average of the Grüneisen number for each mode and direction of propagation is equal to zero for the shear wave. Only the longitudinal wave is responsible for thermoelastic loss because it causes variation in entropy along the direction of propagation. The total attenuation is given as:

$$\left(\alpha/f^2\right)_{\text{Total}} = \left(\alpha/f^2\right)_{Th} + \left(\alpha/f^2\right)_L + \left(\alpha/f^2\right)_S \tag{10}$$

where $\left(\alpha/f^2\right)_L$ and $\left(\alpha/f^2\right)_S$ are the ultrasonic attenuation coefficients due to Akhieser loss for the longitudinal and shear waves respectively.

3. Results and Discussion

For InAs NWs, the basal plane distance (a), axial ratio (p) and density (ρ) are 4.284 Å, 1.633 and 5667 kg·m^{-3} respectively [25]. The calculated values of elastic constants using Equation (2) in present work are shown in **Table 1**. The bulk modulus ($B = \left[2\left(C_{11}+C_{12}\right)+4C_{13}+C_{33}\right]/9$), shear modulus ($G = \left[C_{11}+C_{12}+2C_{33}-4C_{13}+12\left(C_{44}+C_{66}\right)\right]/30$), Young modulus ($Y = 9BG/\left(3B+G\right)$), and Poisson's ratio ($\nu = \left(3B-2G\right)/2\left(3B-G\right)$) of the chosen material are also determined using the SOECs are respectively 51.94 GPa, 35.75 GPa, 87.24 GPa and 0.35. The calculated values of SOECs and the values obtained from the literature [25] are compared in **Table 1**. Thus our calculations of SOECs/TOECs based on only lattice parameters at 300 K are validated. The calculated values of longitudinal, shear and Debye average velocities of ultrasonic wave propagating along the unique axis of the InAs NWs using Equations (3), (4), and (8) and the calculated values of thermal energy density "E_0", specific heat per unit volume "C_V", acoustic coupling constants (D_L and D_S) related with higher order elastic constants through Grüneisen numbers which are functions of SOECs and TOECs using Equation (6) are shown in **Table 2**. It is also clear from **Table 2** that $D_L > D_S$. This implies that the conversion of acoustical energy to thermal energy will be large for wave propagating along the length of wire than the surface wave.

Thermal conductivities of InAs NWs at different diameters (d) taken from the literature [30] are given in **Table 3**. The size (diameter) dependent thermal relaxation time and ultrasonic attenuation coefficients over frequency square under the condition $\omega\tau \ll 1$ are evaluated using Equation (7) and Equations (5), (9), and (10) respectively. They are also listed in **Table 3**. The plots of $\left(a/f^2\right)_{\text{Total}}$ versus diameter of NWs is shown in **Figure 1**. The plot of τ and K versus diameter of NWs is shown in **Figure 2**.

The ultrasonic attenuation coefficients for all sized nanowires and their variation with size are shown in **Figure 1**. The dominant mechanism for total ultrasonic attenuation is $p-p$ interaction. The attenuation due to $p-p$ interaction is directly proportional to the acoustic coupling constant and thermal relaxation time. The ultrasonics velocity is directly related to second order elastic constants while they are related to lattice parameter. The slight

Table 1. SOECs and TOECs in 10^{10} N/m^2 at 300 K.

SOECs	C_{11}	C_{33}	C_{44}	C_{66}	C_{12}	C_{13}
	10.65	11.07	2.74	4.01	2.61	2.29
	10.03*	11.07*	2.30*	2.90*	4.22*	3.18*

TOECs	C_{111}	C_{222}	C_{333}	C_{112}	C_{113}	C_{123}	C_{133}	C_{144}	C_{155}	C_{344}
	−173.61	−137.36	−141.43	−27.53	−5.87	−7.45	−37.39	−8.69	−5.79	−35.05

Table 2. Thermal energy density (E_0: in 10^8 J·m^{-3}), specific heat per unit volume (C_V: in 10^5 J·K^{-1}·m^{-3}), ultrasonic velocities (v_L, v_S and v_D : in 10^3 m·s^{-1}), and acoustic coupling constants (D_L and D_S) for InAs NWs at 300 K.

E_0 (10^8 J·m^{-3})	C_V (10^5 J·K^{-1}·m^{-3})	v_L (10^3 m·s^{-1})	v_s (10^3m·s^{-1})	v_D (10^3m·s^{-1})	D_L	D_S
1.68	7.29	4.42	2.20	2.44	10.38	0.47

Table 3. Size (diameter) dependent thermal conductivity (K), thermal relaxation time (τ) and (α/f^2) for longitudinal and shear wave due phonon-phonon interaction and thermoelastic relaxation mechanisms for InAs NWs at 300 K.

d (nm)	K ($W \cdot m^{-1} \cdot K^{-1}$)	τ (10^{-12} s)	$(\alpha/f^2)_{Th}$ (10^{-18} $Np \cdot s^2 \cdot m^{-1}$)	$(\alpha/f^2)_{Akh.Long}$ (10^{-18} $Np \cdot s^2 \cdot m^{-1}$)	$(\alpha/f^2)_{Akh.Shear}$ (10^{-18} $Np \cdot s^2 \cdot m^{-1}$)	$(\alpha/f^2)_{Total}$ ($\times 10^{-18}$ $Np \cdot s^2 \cdot m^{-1}$)
2.57	4.21	2.91	0.17	273.11	50.20	323.48
3.42	3.91	2.71	0.16	253.65	46.62	300.43
4.28	3.79	2.62	0.15	245.86	45.19	291.20
5.13	3.84	2.66	0.16	249.11	45.79	295.06

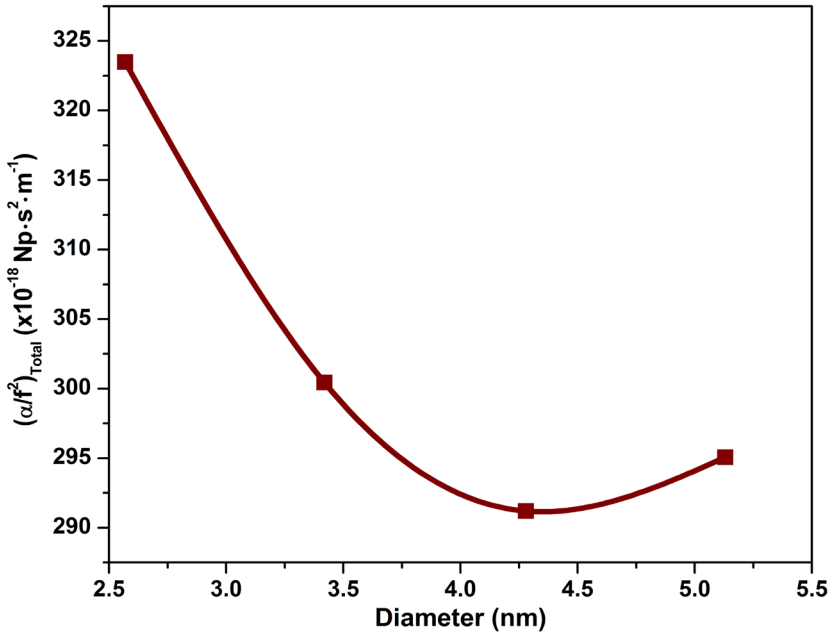

Figure 1. Ultrasonic attenuation of InAs NWs versus diameter at 300 K.

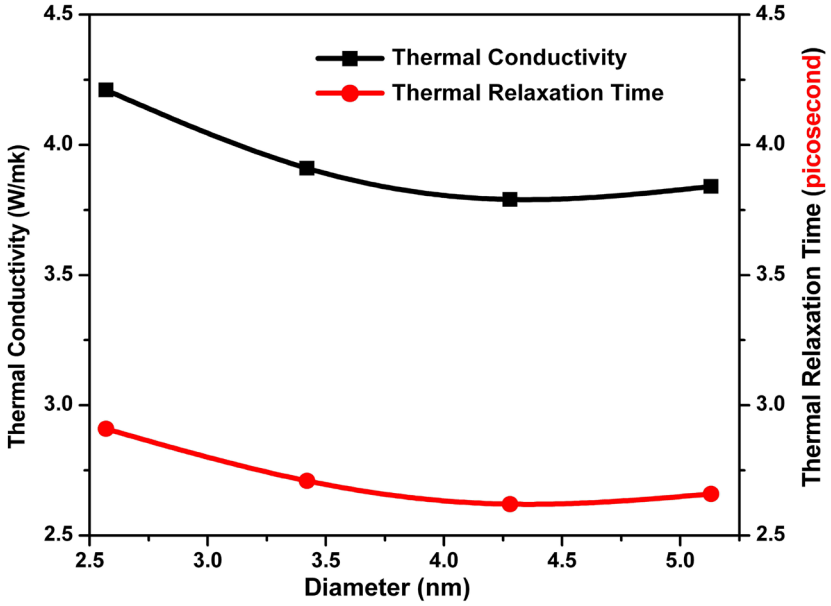

Figure 2. Dependence of thermal conductivity and thermal relaxation time on diameter of InAs NW.

change in velocities, E_0 and C_v for the InAs NW is due to slight change in lattice parameter. In comparison to bulk material the thermal conductivity is lowered at room temperature in the NWs at all diameters. Accordingly the thermal relaxation time is also lowered. It means that the time taken is less for regaining the thermal equilibrium after interaction of the ultrasonic wave with the NWs. Consequently the ultrasonic attenuation in the NWs at frequency ~200 MHz is smaller in comparison to bulk materials [30] [31].

It is clear from **Figure 2** that the variation of the total ultrasonic attenuation coefficient over frequency squares with the diameter of NWs. **Figure 1** follows the same nature as the thermal conductivity or thermal relaxation time. Furthermore, loss of ultrasonic energy for longitudinal wave due to Akhieser damping (phonon-phonon interaction mechanism) is larger than that of shear and other **Table 3**.

Thus on the basis of experimental/calculated data and perusal of **Figure 2** following the above analysis. It is clear that the NWs diameter dependence of the total ultrasonic attenuation is predominantly affected by the unusual low thermal conduction of the NWs. The diameter dependent ultrasonic attenuation curve follows the same pattern as the diameter dependence of thermal conductivity curve at 300 K.

Also, activation energy/crystallinity of nanosized hexagonal structural material decreases/increases with size [32]. The activation energy is well related to resistivity while resistivity is connected with thermal conductivity. Hence decrease in τ with size (diameter) of NWs is attributed to the decrease in crystallinity and increase in activation energy.

However the crystallinity increases beyond 4.5 nm diameter. The size dependency and order of τ approve the semiconducting nature of InAs NWs. [33]. There is deviation from the decreasing behavior of ultrasonic attenuation after 4.5 nm diameter. Thus above the 4.5 nm diameter InAs NW may tend towards its bulk material property.

Thus ultrasonic properties are well correlated with the structure based materials properties depending upon the diameter of the NWs.

4. Conclusion

The simple interaction potential model for the calculations of second and third order elastic constants is validated for the NWs nanowires of different diameters. Theoretical approach for the determination of ultrasonic attenuation in NWs at 300 K with different diameters is established. There is a strong correlation between size dependent ultrasonic attenuation and size dependent thermal conductivity of the NWs. Thus an ultrasonic attenuation mechanism is established to extract the important information about the microstructural phenomena like $p - p$ interaction in the NWs and thermal conductivity behavior with respect to diameters of NWs at 300 K.

Acknowledgements

The authors are thankful to the UGC New Delhi, India for the financial support.

References

[1] Cui, Y., Wei, Q., Park, H. and Lieber, C.M. (2001) Nanowire Nanosensors for Highly Sensitive and Selective Detection of Biological and Chemical Species. *Science*, **293**, 1289-1292. http://dx.doi.org/10.1126/science.1062711

[2] Hahm, J. and Lieber, C.M. (2004) Direct Ultrasensitive Electrical Detection of DNA and DNA Sequence Variations Using Nanowire Nanosensors. *Nano Letters*, **4**, 51-54. http://dx.doi.org/10.1021/nl034853b

[3] Duan, X., Huang, Y., Cui, Y., Wang, J. and Lieber, C.M. (2001) Indium Phosphide Nanowires as Building Blocks for Nanoscale Electronic and Optoelectronic Devices. *Nature*, **409**, 66-69. http://dx.doi.org/10.1038/35051047

[4] Cui, Y., Zhong, Z., Wang, D., Wang, W.U. and Lieber, C.M. (2003) High Performance Silicon Nanowire Field Effect Transistors. *Nano Letters*, **3**, 149-152. http://dx.doi.org/10.1021/nl025875l

[5] Ng, H.T., Han, J., Yamada, T., Nguyen, P., Chen, Y.P. and Meyyappan, M. (2004) Single Crystal Nanowire Vertical Surround-Gate Field-Effect Transistor. *Nano Letters*, **4**, 1247-1452. http://dx.doi.org/10.1021/nl049461z

[6] Persson, A.I., Björk, M.T., Jeppesen, S., Wagner, J.B., Wallenberg, L.R. and Samuelson, L. (2006) $InAs_{1-x}P_x$ Nanowires for Device Engineering, *Nano Letters*, **6**, 403-407. http://dx.doi.org/10.1021/nl052181e

[7] Park, H., Barrelet, C.J., Wu, Y., Tian, B., Qian, F. and Lieber, C.M. (2008) A Wavelength-Selective Photonic-Crystal Waveguide Coupled to a Nanowire Light Source. *Nature Photonics*, **2**, 622-626. http://dx.doi.org/10.1038/nphoton.2008.180

[8] Gong, X.Y., Kan, H., Makino, T., Yamaguchi, T., Nakatskasa, T., Kumagawa, M., Rowell, N.L., Wang, A. and Rinfret,

R. (1995) High Quality $InAs_{1-y}Sb_y$/InAs Multilayers for Mid-IR Detectors. *Crystal Research & Technology*, **30**, 603-612. http://dx.doi.org/10.1002/crat.2170300505

[9] Shenoi, R.V., Attaluri, R.S., Siroya, A., Shao, J., Sharma, Y.D., Stintz, A., Vandervelde, T.E. and Krishna, S. (2008) Low-Strain InAs/InGaAs/GaAs Quantum Dots-in-a-Well Infrared Photodetector. *Journal of Vacuum Science & Technology B*, **26**, 1136-1139. http://dx.doi.org/10.1116/1.2835063

[10] Mou, S., Petschke, A., Lou, Q., Chuang, S.L., Li, J.V. and Hill, C.J. (2008) Midinfrared InAs/GaSb Type-II Superlattice Interband Tunneling Photodetectors. *Applied Physics Letters*, **92**, Article ID: 153505. http://dx.doi.org/10.1063/1.2909538

[11] Huang, Y., Duan, X., Cui, Y., Lauhon, L.J., Kim, K. and Lieber, C.M. (2001) Logic Gates and Computation from Assembled Nanowire Building Blocks. *Science*, **294**, 1313-1317. http://dx.doi.org/10.1126/science.1066192

[12] Wang, J., Gudiksen, M.S., Duan, X., Cui, Y. and Lieber, C.M. (2001) Highly Polarized Photoluminescence and Photodetection from Single Indium Phosphide Nanowires. *Science*, **293**, 1455-1457. http://dx.doi.org/10.1126/science.1062340

[13] Pettersson, H., Trägårdh, J., Persson, A.I., Landin, L., Hessman, D. and Samuelson, L. (2006) Infrared Photodetectors in Heterostructure Nanowires. *Nano Letters*, **6**, 229-232. http://dx.doi.org/10.1021/nl052170l

[14] Law, M., Greene, L.E., Johnson, J.C., Saykally, R. and Yang, P. (2005) Nanowire Dye-Sensitized Solar Cells. *Nature Materials*, **4**, 455-459. http://dx.doi.org/10.1038/nmat1387

[15] Koguchi, M., Kakibayashi, H., Yazawa, M., Hiruma, K. and Katsuyama, T. (1992) Crystal Structure Change of GaAs and InAs Whiskers from Zinc-Blende to Wurtzite Type. *Japanese Journal of Applied Physics Part* 1—*Regular Papers Short Notes & Review Papers*, **31**, 2061-2065.

[16] Martensson, T., Svensson, C.P.T., Wacaser, B.A., Larsson, M.W., Seifert, W., Deppert, K., Gustafsson, A., Wallenberg, L.R. and Samuelson, L. (2004) Epitaxial III-V Nanowires on Silicon. *Nano Letters*, **4**, 1987-1990. http://dx.doi.org/10.1021/nl0487267

[17] Zhou, F. (2009) Thermoelectric Transport in Semiconducting Nanowires. Ph.D. Dissertation, The University of Texas, Austin.

[18] Caroff, P., Dick, K.A., Johansson, J., Messing, M.E., Deppert, K. and Samuelson, L. (2009) Controlled Polytypic and Twin-Plane Superlattices in III-V Nanowires. *Nature Nanotechnology*, **4**, 50-55. http://dx.doi.org/10.1038/nnano.2008.359

[19] Froberg, L.E., Seifert, W. and Johansson, J. (2007) Diameter-Dependent Growth Rate of InAs Nanowires. *Physical Review B*, **76**, Article ID: 153401. http://dx.doi.org/10.1103/PhysRevB.76.153401

[20] Persson, A.I., Froberg, L.E., Jeppesen, S., Bjork, M.T. and Samuelson, L. (2007) Surface Diffusion Effects on Growth of Nanowires by Chemical Beam Epitaxy. *Journal of Applied Physics*, **101**, Article ID: 034313. http://dx.doi.org/10.1063/1.2435800

[21] Yadav, A.K., Yadav, R.R., Pandey, D.K. and Singh, D. (2008) Ultrasonic Study of Fission Products Precipitated in the Nuclear Fuel. *Materials Letters*, **62**, 3258-3261.

[22] Sindhu, S. and Menon, C.S. (1995) Fourth Order Nonlinear Elastic Coefficient of Hexagonal Close Packed Lattice. *Journal of Physics and Chemistry of Solids*, **57**, 1307-1309. http://dx.doi.org/10.1016/0022-3697(95)00323-1

[23] Verma, S.K., Pandey, D.K. and Yadav, R.R. (2012) Size Dependent Ultrasonic Properties of InN Nanowires. *Physica B*: *Condensed Matter*, **407**, 3731-3735. http://dx.doi.org/10.1016/j.physb.2012.05.052

[24] Dhawan, P.K., Wan, M., Verma, S.K., Pandey, D.K. and Yadav, R.R. (2015) Effect of Diameter and Surface Roughness on Ultrasonic Properties of GaAs Nanowires. *Journal of Applied Physics*, **117**, Article ID: 074307. http://dx.doi.org/10.1063/1.4913289

[25] Magnus, W.L., Jakob, B.W., Mathias, W., Håkansson, P., Fröberg, L.E., Samuelson, L. and Wallenberg, L.R. (2007) Strain Mapping in Free-Standing Heterostructured Wurtzite InAs/InP Nanowires. *Nanotechnology*, **18**, Article ID: 015504. http://dx.doi.org/10.1088/0957-4484/18/1/015504

[26] Pandey, D.K., Yadawa, P.K. and Yadav, R.R. (2007) Ultrasonic Properties of Hexagonal ZnS at Nanoscale. *Materials Letters*, **61**, 5194-5198. http://dx.doi.org/10.1016/j.matlet.2007.04.028

[27] Pandey, D.K., Singh, D. and Yadav, R.R. (2007) Ultrasonic Wave Propagation in 3rd Group Nitrides. *Applied Acoustics*, **68**, 766-777. http://dx.doi.org/10.1016/j.apacoust.2006.04.004

[28] Gray, D.E. (1972) American Institute of Physics Handbook. 3rd Edition, McGraw-Hill, New York, 4-58.

[29] Carrete, J., Longo, R.C. and Gallego, L.J. (2011) Prediction of Phonon Thermal Transport in Thin GaAs, InAs and InP Nnowires by Molecular Dynamics Simulations Influence of the Interatomic Potential. *Nanotechnology*, **22**, Article ID: 185704. http://dx.doi.org/10.1088/0957-4484/22/18/185704

[30] Keck, M.J. and Sladek, R.J. (1970) Relaxation Attenuation of Ultrasonic Waves in InAs. *Physical Review B*, **2**, 3135.

http://dx.doi.org/10.1103/PhysRevB.2.3135

[31] Keck, M.J. and Sladek, R.J. (1969) Attenuation of Ultrasonic Waves in InAs at Low Temperatures. *Physical Review*, **185**, 1083. http://dx.doi.org/10.1103/PhysRev.185.1083

[32] Ubale, A.U. and Kulkarni, D.K. (2005) Preparation and Study of Thickness Dependent Electrical Characteristics of Zinc Sulfide Thin Films. *Bulletin of Materials Science*, **28**, 43-47. http://dx.doi.org/10.1007/BF02711171

[33] Yadav, R.R. and Pandey, D.K. (2005) Ultrasonic Properties at the Nanoscale in Some Metals. *Materials Letters*, **59**, 564-569. http://dx.doi.org/10.1016/j.matlet.2004.10.046